Local electronic and geometrical structure of $LaNi_{1-x}Mn_xO_{3+\delta}$ perovskites determined by x-ray-absorption spectroscopy

M. C. Sánchez,[1] J. García,[1,*] J. Blasco,[1] G. Subías,[1,2] and J. Perez-Cacho[1]
[1]*Instituto de Ciencia de Materiales de Aragón and Departamento de Física de la Materia Condensada, Consejo Superior de Investigaciones Científicas y Universidad de Zaragoza, 50009 Zaragoza, Spain*
[2]*European Synchrotron Radiation Facility, Boîte Postale 220, 38043 Grenoble, France*
(Received 5 June 2001; revised manuscript received 24 September 2001; published 22 March 2002)

Local and electronic structures of Ni and Mn atoms in the $LaNi_{1-x}Mn_xO_{3+\delta}$ series were studied by means of x-ray-absorption spectroscopy. The Ni and Mn K edges and Mn L_3/L_2 edges were analyzed. The local structure, determined by extended x-ray-absorption fine-structure spectroscopy, shows a distorted MnO_6 octahedron in $LaMnO_3$. This distortion decreases when Ni replaces Mn in the unit cell. In samples with the same Mn/Ni ratio, the octahedron distortion is smaller in oxidized samples. This result shows that the holes induced by oxidation belong mainly to the Mn sublattice. In the $LaNi_{1-x}Mn_xO_{3+\delta}$ series, a contraction of the MnO_6 octahedron is coupled to an expansion of the NiO_6 octahedron. This result is well correlated with the changes in the oxidation states deduced from x-ray-absorption near-edge spectroscopy (XANES). The Mn valence state continuously changes from the formal 3+ state in $LaMnO_3$ to nearly a 4+ state in $LaNi_{0.5}Mn_{0.5}O_3$. The Ni valence state instead shifts from Ni^{3+} in $LaNiO_3$ to Ni^{2+} in $LaNi_{0.5}Mn_{0.5}O_3$. Therefore, Ni^{2+} and Mn^{4+} are present in $LaNi_{0.5}Mn_{0.5}O_{3+\delta}$. Moreover, the detailed analysis of the XANES spectra points to an important mixing between the $3d$ orbitals of both cations and the $2p$ orbitals of oxygen atoms.

DOI: 10.1103/PhysRevB.65.144409 PACS number(s): 61.10.Ht, 78.70.Dm, 75.50.Dd, 71.28.+d

I. INTRODUCTION

The doping of transition-metal (TM) oxides with perovskite structure induces remarkable phenomena such as superconductivity, giant magnetoresistance, or metal-insulator transitions.[1] Moreover, the discovery of exotic properties in $R_{1-x}A_xMnO_3$ (R=rare earth, A=divalent cation) compounds has stimulated the research in other oxides where Mn is in a mixed-valence state.[2] Thus, $LaM_{1-x}Mn_xO_3$ (M=Ni,Co) are ferromagnets[3] and their magnetic ordering was explained[4] in terms of a positive superexchange interaction between Ni^{2+} (or Co^{2+}) and Mn^{4+}. Magnetic measurements and NMR studies seem to support this description.[5,6] However, for the case of the $LaNi_{1-x}Mn_xO_3$ series, other authors[7,8] claim instead for the presence of a homovalent substitution between Mn^{3+} and Ni^{3+}. Even more, some of them ascribed these differences to synthetic details.[7] Finally, a recent spectroscopy study[9] on $LaMn_{1-x}Co_xO_3$ compounds suggests that there is a mixture of Mn^{+3} and Mn^{4+} in this series and that a double-exchange mechanism[10] is required to account for the ferromagnetism of these samples. Therefore, a controversy actually exists about the electronic state of transition metals in this family of compounds.

We have recently studied the $LaNi_{1-x}Mn_xO_3$ series by means of diffraction techniques.[11,12] We have observed perovskite single phases for the whole series and not only for $x \geq 0.5$, as was reported in the past.[5,13] Neutron-diffraction measurements strongly suggest the ordered arrangement of Ni and Mn atoms in the $LaNi_{0.5}Mn_{0.5}O_3$ composition, but for the rest of the samples a random Ni/Mn distribution is deduced.[12] This fact makes it very difficult to determine the electronic states by means of diffraction techniques. Since the knowledge of the TM electronic states in oxides is an important key to understand their properties we must pursue this objective. In fact, though these oxides have traditionally been described as pure ionic compounds, recent experiments on mixed-valence oxides, such as magnetite[14] or manganites,[15] are casting doubts on the accuracy of a simple ionic model to properly describe TM oxides.

In this paper, we report on an x-ray-absorption spectroscopy study of the $LaNi_{1-x}Mn_xO_{3+\delta}$ ($0 \leqslant x \leqslant 1$) series at Mn ($K$ and L_3/L_2) and Ni (K) edges. The aim of this work is twofold: First, we have used extended x-ray-absorption fine-structure (EXAFS) spectroscopy to separately extract the local geometric structure around each TM atom. Second, we have studied the electronic state and local geometry by means of x-ray-absorption near-edge spectroscopy (XANES). The TM K-edge spectrum provides information about the local geometry around TM's, the TM valence state, and the covalence between O-$2p$ and TM $3d$ states. Moreover, the TM L_3/L_2-edge spectra provide direct information on the TM $3d$ states. Since both techniques, EXAFS and XANES, are complementary, we have correlated the different EXAFS and XANES features observed. Finally, we have studied samples prepared from different synthetic routes, to check how the preparation method affects the local and electronic structures.

II. EXPERIMENT

The study is focused on $LaNi_{1-x}Mn_xO_{3+\delta}$ (x=0, 0.1, 0.25, 0.5, 0.75, 0.9, and 1) samples. The synthetic route and crystallographic structure have been reported elsewhere.[12,16,17] All samples were characterized as single-phase perovskites by x-ray powder diffraction at room temperature. Thermogravimetric analysis in a reducing atmosphere (Ar/H_2=95/5) was used to determine the oxygen content of the samples. Table I summarizes the space group and oxygen content for the samples studied in this work. The $LaNi_{0.5}Mn_{0.5}O_{3+\delta}$ samples show a structural phase transition between 270 and 315 K, and therefore, the low- and high-

TABLE I. Space groups and oxygen content of $LaNi_{1-x}Mn_xO_{3+\delta}$ samples and $CaMnO_3$. These space groups are taken as a rough approximation (*). The ordered arrangement of Ni and Mn atoms in these samples implies a symmetry reduction of the crystallographic cell (probably $P2_1/n$ and $R\bar{3}m$ instead of *Pbnm* and $R\bar{3}c$).

Sample	Space group	Unit cell		
		a	*b*	*c*
$LaMnO_3$	*pbnm*	5.535	5.723	7.697
$LaNi_{0.1}Mn_{0.9}O_3$	*pbnm*	5.531	5.582	7.788
$LaNi_{0.1}Mn_{0.9}O_{3.13}$	$R\bar{3}c$	5.521		13.327
$LaNi_{0.25}Mn_{0.75}O_{2.97}$	*pbnm*	5.531	5.504	7.792
$LaNi_{0.25}Mn_{0.75}O_{3.09}$	*pbnm*	5.520	5.471	7.757
$LaNi_{0.5}Mn_{0.5}O_{3.05}$*	*pbnm* (68%)	5.512	5.458	7.739
	$R\bar{3}c$ (32%)	5.513		13.236
$LaNi_{0.5}Mn_{0.5}O_{3.08}$*	$R\bar{3}c$ (66%)	5.504		13.237
	pbnm (34%)	5.502	5.450	7.736
$LaNi_{0.75}Mn_{0.25}O_3$	$R\bar{3}c$	5.480		13.198
$LaNi_{0.9}Mn_{0.1}O_{3.02}$	$R\bar{3}c$	5.462		13.165
$LaNiO_3$	$R\bar{3}c$	5.457		13.146
$CaMnO_3$	*pbnm*	5.268	5.281	7.458

temperature phases coexist at room temperature (see Table I).

X-ray-absorption measurements at the metal *K* edge were carried out at beamlines 7.1 and 8.1 at the Synchrotron Radiation Source (Daresbury) and at beamline ID26 at the European Synchrotron Radiation Facility (Grenoble). The Daresbury storage ring was operated at 2 GeV, with an average current of 150 mA. The ESRF storage ring was operated at 6 GeV with a maximum stored current of about 190 mA. To monochromatize the radiation a double Si (111) crystal was used; harmonic rejection was performed by slightly detuning the two crystals except for beamline ID26, where a setup of mirrors was used. The energy resolution, $\Delta E/E$, was estimated to be about 2×10^{-4}. Ionization chambers were used to detect the incident and transmitted flux at SRS, whereas silicon photodiodes were used at ESRF. The absorption spectra were recorded in the transmission mode at room temperature. At the Mn *K* edge, spectra were also recorded in the fluorescence mode. Equivalent spectra were obtained in both cases, which allows us to discard any significant contribution arising from the La L_1 edge.

The $LaMnO_3$, $CaMnO_3$, and $LaNi_{0.5}Mn_{0.5}O_3$ Mn L_3/L_2-edge spectra were measured at the beamline ID12B (presently, ID8) at the ESRF. Spectra were recorded in the total electron yield mode.

The experimental XANES and EXAFS signals have been extracted from the raw data following standard procedures,[18] namely, background removal was performed and the atomic absorption coefficient was determined by a low-order polynomial fit of the spectra. After background subtraction XANES spectra were normalized to high energy (around 100 eV above the absorption edge).

III. RESULTS

A. EXAFS study

Figure 1(a) shows the room-temperature Mn *K*-edge EXAFS spectra for selected samples. From $LaMnO_3$ to $LaNi_{0.75}Mn_{0.25}O_3$ a continuous evolution in the oscillations of the spectra is observed. Figure 1(b) displays the Fourier transform, taken between 2.8 and 12 $Å^{-1}$, of the EXAFS spectra. The intensity of both the first and second peaks rises as the Mn content decreases. Since the first peak is related to the first oxygen coordination shell, the peak intensity increase nicely agrees with a reduction of the distortion of the MnO_6 octahedra, because the Mn-O coordination remains constant along the whole series.[12] This is true even for the oxidized samples, where the oxygen excess implies TM vacancies, not interstitial oxygen. The reduction of the MnO_6 distortion can be ascribed both to the disappearance of the static Jahn-Teller distortion of the $LaMnO_3$ and to the diminution of the orthorhombic distortion in the unit cell with decreasing Mn content (see Table I). For the $LaNi_{1-x}Mn_xO_{3+\delta}$ samples with $x\leqslant0.5$ it is worth remembering that they show a rhombohedral unit cell with only one TM-O distance (i.e., a regular MnO_6 octahedron). The intensity increase of the second peak (related to the second coordination shell) as the Mn content decreases [see Fig. 1(b)] can also be associated with the decrease of the orthorhombic distortion of the crystallographic cell.

Figure 2(a) and 2(b) show the Ni *K*-edge EXAFS spectra of selected samples and their Fourier transform (FT) taken from 2.8 to 12 $Å^{-1}$, respectively. Again a continuous evolution of the EXAFS oscillation from $LaNiO_3$ to $LaNi_{0.25}Mn_{0.75}O_{3.09}$ is observed. Moreover, the position of the FT first peak shifts toward higher values as the Mn content increases. This result indicates an increase of the Ni-O distance with increasing Mn content.

To investigate the local oxygen environment around both of the TM atoms, the EXAFS contribution of the first shell was extracted by Fourier filtering the spectra between 1 and 2 Å. By least-squares fitting the *k*-weighted filtered spectra in the range $3<k<11.5$ $Å^{-1}$ we obtained the information

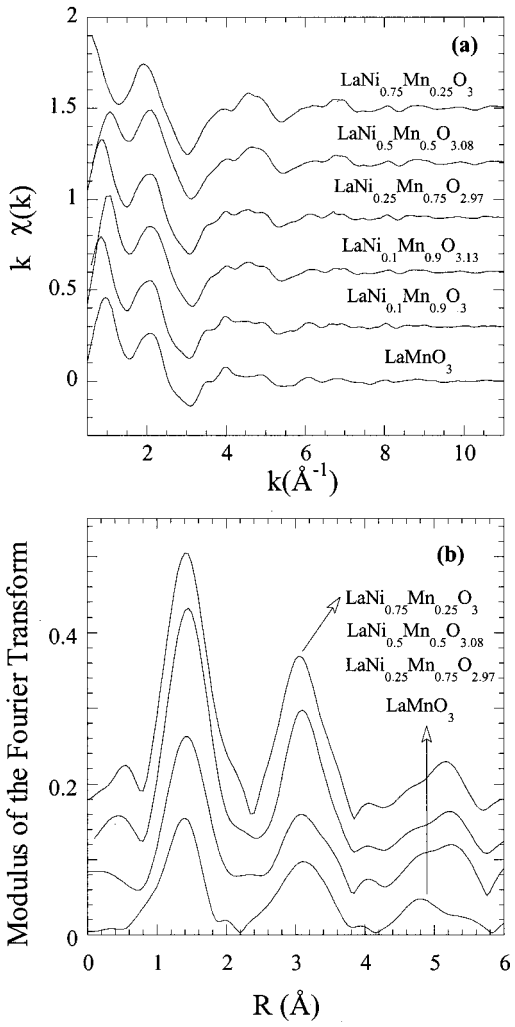

FIG. 1. (a) *k*-weighted EXAFS spectra at the Mn *K* edge of $LaNi_{1-x}Mn_xO_{3+\delta}$ samples (indicated in the figure). (b) Modulus of the Fourier transform of the Mn *K*-edge EXAFS spectra for selected samples.

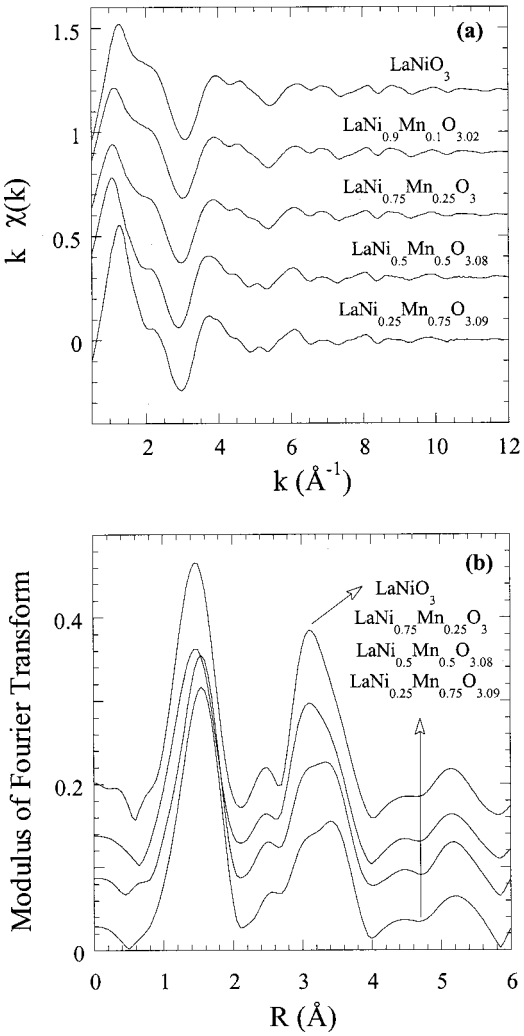

FIG. 2. (a) *k*-weighted EXAFS spectra at the Ni *K* edge of selected $LaNi_{1-x}Mn_xO_{3+\delta}$ samples (indicated in the figure). (b) Modulus of the Fourier transform of the Ni *K*-edge EXAFS spectra for selected samples.

about Mn-O and Ni-O bond distribution. For the sake of comparison and for some selected samples, the best-fit results are displayed in Fig. 3. We used the Mn-O pair signal extracted from the experimental $CaMnO_3$ EXAFS spectrum and the Ni-O pair signal extracted from the experimental $LaNiO_3$ EXAFS spectrum as references. We analyzed the spectra of these samples using the theoretical phases and amplitudes generated from the FEFF code.[19] The best-fit parameters, which correspond to the best-fit simulations of the first coordination shell, are summarized in Table II. We point out that for stoichiometric $LaMnO_3$ the static Jahn-Teller distortion is well resolved, in agreement with previous data.[20] For the rest of the samples we have used a single Mn-O distance model (coordination fixed to 6) to analyze the first coordination shell. Since the value of the Debye-Waller (DW) factor is related to the Mn-O distances spread, samples with MnO_6 distorted octahedron[20,21] show large DW factors (for instance, see the value for $LaNi_{0.1}Mn_{0.9}O_3$ in Table II). In general, the Mn-O distances and the DW factors values decrease with the Mn content. This decrease is correlated with the oxidation degree of Mn atoms. It is worth remembering that the ionic radius[22] for Mn^{4+} is 0.115-Å smaller than for Mn^{3+}. We have also studied samples with the same Ni/Mn composition, but with different oxygen content. We have found smaller DW factor values and smaller Mn-O distances for oxidized samples, which suggests an increase of holes (oxidation) of the Mn sublattice. We have also noted the presence of small DW factor values in the fits of $LaNi_{0.75}Mn_{0.25}O_3$ and $LaNi_{0.5}Mn_{0.5}O_{3.08}$ samples. These DW factor values are even smaller than that of $CaMnO_3$. This result agrees with the presence of a regular MnO_6 octahedron in the former samples, with a rhombohedral cell, whereas the latter instead shows an orthorhombic unit cell with different Mn-O distances. However, another possibility could be the change in the correlated Debye temperature for the $Ni_{0.5}Mn_{0.5}$ system.

Table II also summarizes the results obtained for the Ni atom local environment. We observe an increase of the Ni-O distance as the Mn content increases. This is also in agree-

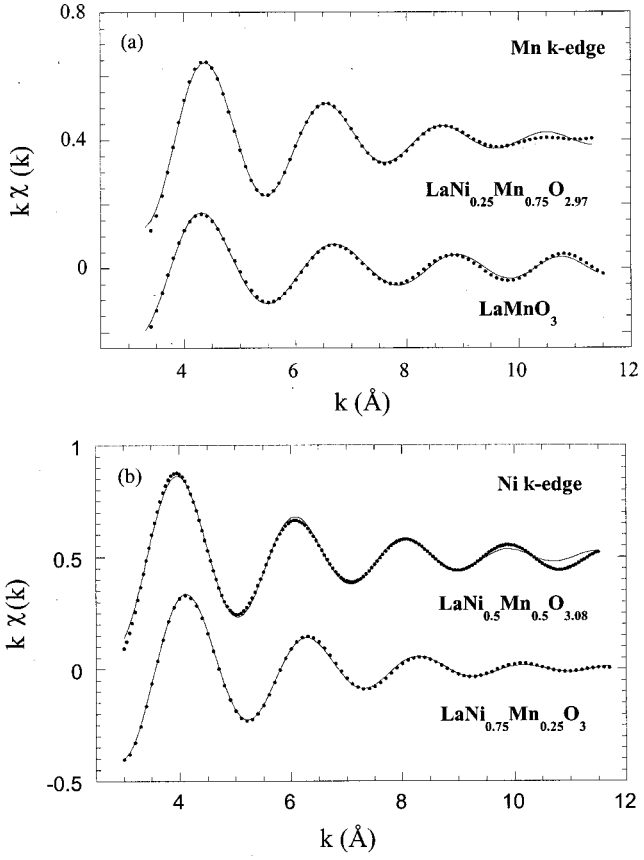

FIG. 3. Comparison between Fourier filtered first shell experimental spectra (points) and best-fit simulation (lines) for (a) $LaMnO_3$ and $LaNi_{0.25}Mn_{0.75}O_{2.97}$ samples at the Mn *K* edge and (b) $LaNi_{0.5}Mn_{0.5}O_{3.08}$ and $LaNi_{0.75}Mn_{0.25}O_3$ samples at the Ni *K* edge.

ment with a reduction of the Ni oxidation state when the Mn content increases (it is noteworthy that Ni^{2+} has an ionic radius[22] rather larger than Ni^{3+}). Therefore, for the $LaNi_{0.5}Mn_{0.5}O_{3.08}$ different local environments are observed for Mn and Ni atoms.

Finally, the $LaNi_{0.75}Mn_{0.25}O_3$ sample has an anomalous high DW factor value for the first coordination Ni atom shell (see Table II). This fact could indicate the presence of some kind of distortion around the Ni atom, distortion which is also observed at low temperatures. The DW factor value decreases with decreasing temperature, but its value at 30 K is larger than the one observed for the rest of the samples at room temperature (Table II). Previous studies state that $LaNi_{1-x}Mn_xO_{3+\delta}$ samples with $x<0.5$ are actually a mixture of $LaNiO_3$ and $LaNi_{0.5}Mn_{0.5}O_3$. Such phase segregation could explain the large DW factor found for $LaNi_{0.75}Mn_{0.25}O_3$. However, transmission electron microscopy has determined the existence of a unique phase for the last cited compound, which discards the presence of two different crystallographic phases in $LaNi_{0.75}Mn_{0.25}O_3$. Therefore, the origin of this anomalous DW factor should be ascribed to a local inhomogeneity not detected by diffraction studies.

TABLE II. EXAFS parameters of the first oxygen coordination shell for $LaNi_{1-x}Mn_xO_{3+\delta}$ samples. *N* are the coordination number, and *D* are the interatomic Mn-O (or Ni-O) distances. σ^2 are the absolute values for the Debye-Waller factors. *R* is the best-fit residual factor normalized by the difference between the number of independent points of the spectra and the number of fit parameters (Ref. 24). Estimated errors for Mn-O and Ni-O bonds are ± 0.01 Å. Numbers in parentheses are statistical errors of the last significant digit.

Sample	*N*	*D* (Å)	$\sigma^2\times10^{-3}$ (Å^2)	*R*
Mn *K* edge				
$LaMnO_3$	4	1.94	1.3(6)	0.01
	2	2.17	10(2)	
$LaNi_{0.1}Mn_{0.9}O_{3.13}$	6	1.94	4.1(6)	0.03
$LaNi_{0.1}Mn_{0.9}O_3$	6	1.95	7.7(6)	0.007
$LaNi_{0.25}Mn_{0.75}O_{2.97}$	6	1.95	3.8(5)	0.007
$LaNi_{0.5}Mn_{0.5}O_{3.08}$	6	1.92	0.1(5)	0.02
$LaNi_{0.75}Mn_{0.25}O_3$	6	1.92	0.4(5)	0.07
$CaMnO_3$	6	1.92	1.5(2)	0.002
Ni *K* edge				
$LaNiO_3$ (300 K)	6	1.93	3.6(6)	0.002
(80 K)	6	1.93	2.8(6)	0.002
$LaNi_{0.9}Mn_{0.1}O_{3.02}$	6	1.93	4.2(6)	0.0015
$LaNi_{0.75}Mn_{0.25}O_3$(300 K)	6	1.95	6.0(7)	0.002
(200 K)	6	1.94	5.6(6)	0.002
(100 K)	6	1.94	5.1(6)	0.002
(30 K)	6	1.94	4.9(6)	0.002
$LaNi_{0.5}Mn_{0.5}O_{3.08}$	6	2.01	3.6(6)	0.003

B. XANES study

The Mn *K*-edge room-temperature XANES spectra of $LaNi_{1-x}Mn_xO_{3+\delta}$ ($x=0.25$, 0.5, 0.75, 0.9, and 1) samples are shown in Fig. 4. The spectrum of $CaMnO_3$ is also showed as a reference. All of these spectra are very similar to each other and, furthermore, they are very similar to the mixed-valence manganites spectra reported elsewhere,[15,21] as expected for compounds with a similar perovskite structure. The spectra are characterized by two resonances: a main resonance at the edge (denoted by A) and a second resonance (B) beyond the edge. They also show a complicated prepeak structure, displayed in the insets of the Fig. 4. The main difference among the spectra is the energy position of the absorption edge. Figure 4(a) shows that from $LaMnO_3$ to $LaNi_{0.5}Mn_{0.5}O_{3+\delta}$ there is a continuous shift of the edge to higher energies. Figure 4(b) shows instead the absence of a chemical shift between $LaNi_{0.5}Mn_{0.5}O_{3+\delta}$ and $LaNi_{0.75}Mn_{0.25}O_3$ samples. This result suggests a similar electronic charge for the Mn atoms in $LaNi_{1-x}Mn_xO_3$ samples with $x\leqslant 0.5$. In any case, the edge position for these samples lies at lower energy than for $CaMnO_3$.

It is well known that, for manganites, the position of the absorption edge can be correlated with the valence state of Mn atoms.[15,21] If the absorption edge position (E_0) is taken as the inflection point of the edge, we have calculated the

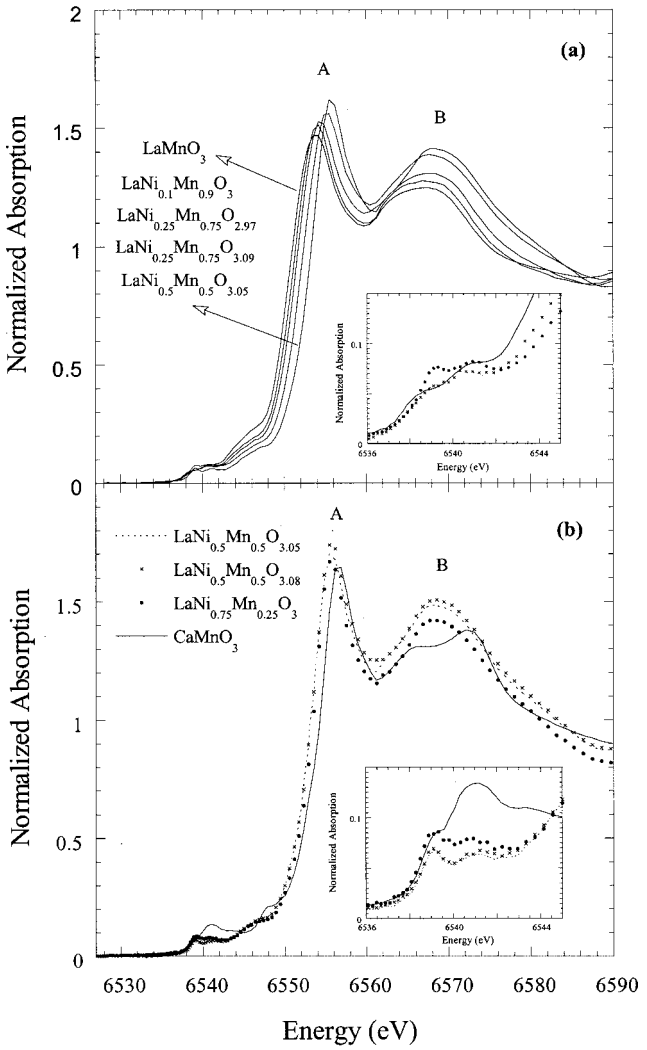

FIG. 4. (a) Normalized Mn *K*-edge XANES spectra for $LaNi_{1-x}Mn_xO_{3+\delta}$ compounds with $x \geq 0.5$. Inset: Preedge region of the XANES spectra for $LaMnO_3$ (line), $LaNi_{0.25}Mn_{0.75}O_{2.97}$ (crosses), and $LaNi_{0.25}Mn_{0.75}O_{3.09}$ (points). (b) Normalized Mn *K* edge XANES spectra of $LaNi_{1-x}Mn_xO_{3+\delta}$ compounds with $x \leq 0.5$ compared to the $CaMnO_3$ spectrum. Inset: Preedge region for the same compounds.

chemical shift (ΔE_0) between $LaMnO_3$ and the rest of the samples. The results are summarized in Table III. First, ΔE_0 is 4.3 eV for $CaMnO_3$, i.e., between Mn^{3+} and Mn^{4+}) in agreement with reported data.[15,21] If a linear relationship between ΔE_0 and the valence state is considered, we can evaluate the oxidation state for Mn atoms and this comparison is established in Fig. 5. The valence of Mn atoms increases up to $(1-x)=0.5$. At this point, the system seems to achieve its maximum oxidation state. For samples with the same Ni/Mn ratio and different δ, the oxidation state of Mn atoms increases with δ. Both results agree with the local structure determination as previously described in the EXAFS study.

The preedge region exhibits a complicated structure, which depends on the Ni/Mn ratio (see insets of Fig. 4). Thus, the preedge regions of $LaMnO_3$ and $LaMn_{0.9}Ni_{0.1}O_3$ clearly show two peaks, as reported elsewhere,[5] but the prepeak structures change for samples with a higher content of Ni. Moreover, a plateaulike shape is observed for $x<0.75$ samples, though two peaks are still visible. Finally, the oxidation degree of the samples also affects the prepeak structure, which is evident, for instance, from the inset of Fig. 4(a), which compares the prepeak region for $LaNi_{0.25}Mn_{0.75}O_{2.97}$ and $LaNi_{0.25}Mn_{0.75}O_{3.09}$. For the latter compound, the intensity of the peak located at 6539 eV increases and since this sample has a less distorted structure (see Table I), this feature could be related to an increase of the mixing between $3d$ and $2p$ states. Another important result is displayed in the inset of Fig. 4(b), where we compare the preedge regions of $CaMnO_3$, $LaNi_{0.5}Mn_{0.5}O_3$, and $LaNi_{0.75}Mn_{0.25}O_3$ samples, with nominal Mn^{4+}. The inset in Fig. 4(a) shows a different prepeak structure for $CaMnO_3$ than for the Ni compounds, which suggests a different mixing between Mn-$3d$ and O-$2p$ states.

Figure 6 shows the normalized XANES spectra at the Ni *K* edge for $LaNi_{1-x}Mn_xO_{3+\delta}$ samples. The $LaNiO_3$ spectrum is also characterized by two resonances: a main resonance at the edge (A′) and a second one beyond the edge (B′). In addition, the preedge region shows only one prepeak [see inset of Fig. 6(b)]. Both $LaNi_{0.9}Mn_{0.1}O_{3.02}$ and $LaNi_{0.75}Mn_{0.25}O_3$ have the same features in their spectra. However, strong changes are observed for the $LaNi_{0.5}Mn_{0.5}O_{3.05}$ spectrum. First, a shoulder (denoted as C) is clearly observed between resonances A′ and B′ and second, the preedge peak is split. These features are also observed in the $LaNi_{0.25}Mn_{0.75}O_{2.97}$ spectrum. Therefore, the strong change in the electronic state of Ni atoms is observed at $x \approx 0.5$, which coincides with a change in the crystallographic structure[12] (see Table I). Although the spectra were normalized well beyond the absorption edge, the value of the white line (peak A) is alike for all of them.

We have also studied the chemical shift in the Ni *K*-edge spectra. In this case, ΔE_O is calculated with respect to the $LaNiO_3$ spectrum. ΔE_O ranges from 0.6 eV for $x<0.5$ to up to 1.1 eV for $x \geq 0.5$ samples. Bearing in mind that ΔE_O between Ni^{3+} and Ni^{2+} is less[23,24] than 2 eV, this result suggests an oxidation state close to +2 for Ni atoms in samples with $x \geq 0.5$. Furthermore, the strong change observed in the XANES spectra at $x \approx 0.5$ might indicate, as a rough approximation, that Ni is +2 for $x \geq 0.5$ and that it is in a mixed-valence state for $x<0.5$. However, it is noteworthy that the double peak observed for $LaNi_{1-x}Mn_xO_3$ ($x \geq 0.5$), see inset of Fig. 6(a), is not observed in other Ni^{2+} oxides,[23,24] which indicates for this system a different degree of hybridization between Ni-$3d$ and O-$2p$ states.

Our above-described results seem to point out for $LaNi_{0.5}Mn_{0.5}O_{3+\delta}$ that Ni^{+2} and Mn^{+4} may be, most probably, the oxidation states. To verify it, XANES spectra at the Mn L_3/L_2 edges were measured for $LaNi_{0.5}Mn_{0.5}O_{3.05}$, $LaMnO_3$, and $CaMnO_3$. The results are displayed in Fig. 7. The $LaMnO_3$ spectrum perfectly agrees with previous measurements reported elsewhere,[25] whereas the $CaMnO_3$ spectrum is very similar to that reported[25] for $La_{0.1}Sr_{0.9}MnO_3$. These spectra provide direct information about the TM $3d$ states because the most intense structure corresponds to tran-

TABLE III. Threshold energies (E_0) and chemical shifts (ΔE_0) for the $LaNi_{1-x}Mn_xO_{3+\delta}$ series and the reference compound $CaMnO_3$ at room temperature.

Sample	Mn *K* edge E_0 (eV)	ΔE_0 (eV)	Ni *K* edge E_0 (eV)	ΔE_0 (eV)
$LaMnO_3$	6550.5	0.0		
$LaNi_{0.1}Mn_{0.9}O_3$	6551.1	0.6		
$LaNi_{0.1}Mn_{0.9}O_{3.13}$	6551.7	1.2		
$LaNi_{0.25}Mn_{0.75}O_{2.97}$	6551.7	1.2	8346.3	1.1
$LaNi_{0.25}Mn_{0.75}O_{3.09}$	6552.3	1.8	8346.3	1.1
$LaNi_{0.5}Mn_{0.5}O_{3.05}$	6553.8	3.3	8346.3	1.1
$LaNi_{0.5}Mn_{0.5}O_{3.08}$	6553.8	3.3	8346.3	1.1
$LaNi_{0.75}Mn_{0.25}O_3$	6553.8	3.3	8346.8	0.6
$LaNi_{0.9}Mn_{0.1}O_{3.02}$			8346.8	0.6
$LaNiO_3$			8347.4	0.0
$CaMnO_3$	6554.8	4.3		

sitions of the form $2p \rightarrow 3d$, as dictated by the dipole selection rule. The edge positions coincide for the $CaMnO_3$ and $LaNi_{0.5}Mn_{0.5}O_{3.05}$ spectra, which suggests that in both compounds the Mn atoms have a similar electronic configuration. In addition, both spectra show similar features, but they are quite different from those observed in the $LaMnO_3$ spectrum. The only difference between the $CaMnO_3$ and $LaNi_{0.5}Mn_{0.5}O_{3.05}$ spectra arises from a broadening of the spectral lines. This broadening is not an experimental artifact, because both spectra were measured in the same conditions. Some authors[25] argued that spectral broadening depends on several factors: the $3d$ bandwidth, the covalent character of the ground state, and the symmetry around the absorbing atoms. Therefore, the different broadening can be related to differences in some of these factors. For instance, the Mn-$3d$ band is expected to be broader for $CaMnO_3$ or the symmetry around Mn ions is higher for $LaNi_{0.5}Mn_{0.5}O_{3.05}$ (rhombohedral cell).

IV. DISCUSSION AND CONCLUSIONS

Though the $LaNi_{1-x}Mn_xO_3$ series was extensively studied in the past, several questions still remain open. The most

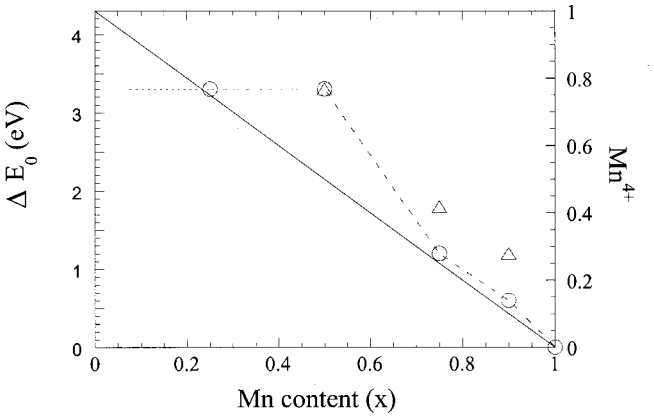

FIG. 5. Chemical shift (ΔE_0) and hole count (Mn^{4+}) as a function of the Mn content. Circles are used for nearly stoichiometric samples and triangles for samples with oxygen excess.

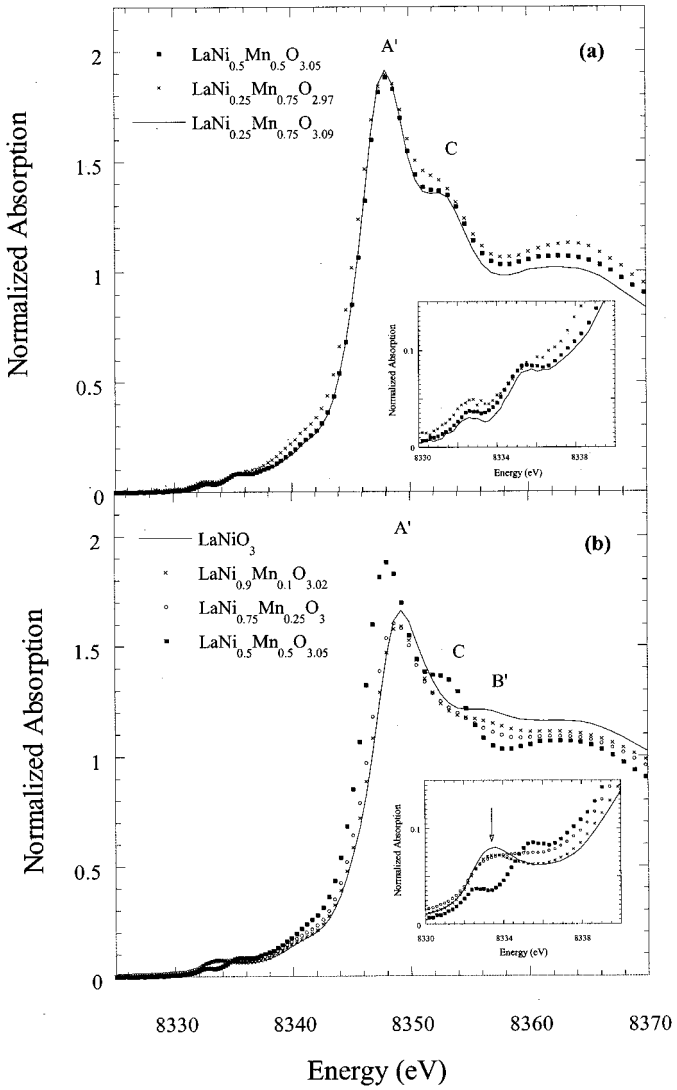

FIG. 6. Normalized Ni *K*-edge XANES spectra of $LaNi_{1-x}Mn_xO_{3+\delta}$ compounds: (a) spectra of compounds with $x \geqslant 0.5$; (b) spectra for $x \leqslant 0.5$. The insets show the preedge region for the respective compounds.

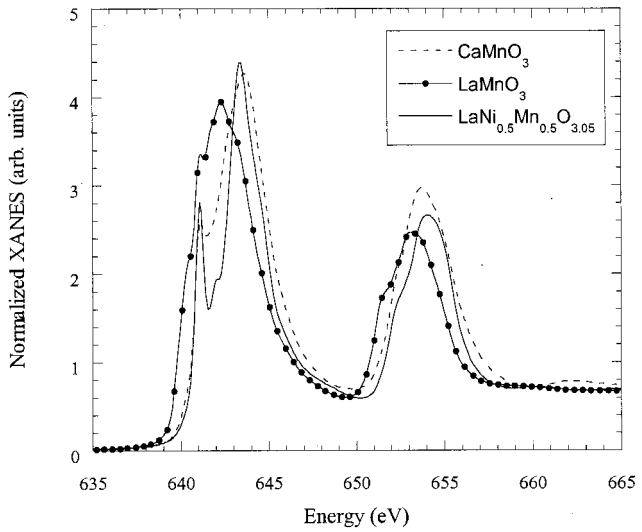

FIG. 7. Normalized Mn L_3/L_2-edge XANES spectra of $CaMnO_3$, $LaMnO_3$, and $LaNi_{0.5}Mn_{0.5}O_{3.05}$ samples.

important point refers to the problem of the valence ambiguity of this system. Thus, it is known that, depending on several factors, the equilibrium $Ni^{2+}+Mn^{4+}\rightleftarrows Ni^{3+}+Mn^{3+}$ may be driven either to the left or to the right. Moreover, in the literature there is some controversy about the electronic states chosen for this system, either on the left[3–6] side or on the right[7,8] side of the reaction above.

The parent compounds $LaMnO_3$ and $LaNiO_3$ show Mn^{+3} and Ni^{+3} ions, respectively. Our EXAFS results indicate that the replacement of Mn by Ni in $LaMnO_3$ first produces a reduction of the local tetragonal distortion of the MnO_6 octahedron and second a decrease of the average Mn-O distances. These changes suggest the diminution of the Mn^{3+} (a Jahn-Teller ion) content when the Ni content increases. This agrees with the chemical shift observed in the Mn *K*-edge XANES spectra. Accordingly, the opposite effects are noticed at the Ni *K* edge: the substitution of Ni by Mn in $LaNiO_3$ produces an increase in the average Ni-O distance, and the chemical shift of the Ni *K*-edge XANES spectra suggests the reduction of Ni^{3+}. Therefore, the reaction above seems to be driven to the left. The process would be completed at the midpoint of the series, i.e., $LaMn_{0.5}Ni_{0.5}O_{3+\delta}$ should be composed of Ni^{2+} and Mn^{4+}. The interatomic distances calculated from EXAFS spectroscopy agree with this description, which shows that, for $LaMn_{0.5}Ni_{0.5}O_{3+\delta}$ samples, the NiO_6 octahedron is greater than the MnO_6 one. This could be the driving force for a partial Mn/Ni ordering of these atoms in the perovskite lattice. This ordering was proposed in the past[4] and it has recently been detected by neutron-diffraction experiments.[12] Therefore, $LaNi_{0.5}Mn_{0.5}O_3$ can be considered as a double perovskite,[26] i.e., La_2NiMnO_6.

The $LaNi_{0.5}Mn_{0.5}O_{3+\delta}$ XANES spectrum qualitatively agrees with this picture. ΔE_0 for the Mn *K* edge gives a valence state of +3.8, very close to the ideal value of +4. This deviation could indicate either that the reaction above is not fully driven to the left or that the linear relationship between ΔE_0 and the valence state does not perfectly work for this particular system (details such as the different local geometry between $CaMnO_3$ and $LaNi_{0.5}Mn_{0.5}O_3$ must also be taken into account). The latter argument seems to be more plausible, because the Mn L_3/L_2-edge spectra suggest a very similar electronic state for Mn atoms in $CaMnO_3$ and $LaNi_{0.5}Mn_{0.5}O_3$. Nevertheless, it is worth realizing that even if Ni and Mn are considered as +2 and +4, respectively, they have their own particular features in $LaNi_{0.5}Mn_{0.5}O_3$. For instance, the preedge structures in the XANES spectra of both edges suggest a particular mixing of $3d$ and $2p$ states for this system, different from the one for other perovskite oxides.

The rest of the samples also show interesting features. The XANES spectra for the Mn *K* edge (Ni *K* edge) in the Ni-rich region (Mn-rich region) seem to be identical to that observed for the $LaNi_{0.5}Mn_{0.5}O_{3+\delta}$ sample. Consequently, the electronic states seem to be very similar. However, several differences are observed in the spectra of the Mn *K* edge (Ni *K* edge) in the Mn-rich region (Ni-rich region). There are two possibilities for these compounds. The mixed Mn^{+3}/Mn^{+4} valence state in the Mn-rich region (Ni^{+3}/Ni^{+2} in the Ni-rich region) can be either a distribution of Mn^{+3} and Mn^{+4} (Ni^{+3} and Ni^{+2}) ions or an intermediate-valence state $Mn^{3.\eta+}$ ($Ni^{2.\eta+}$). Note that for the $LaNi_{1-x}Mn_xO_{3+\delta}$ series the value of η depends on both the doping ratio x and the oxygen content δ.

One of the basic principles of x-ray-absorption spectroscopy states that the absorption spectrum is the incoherent addition of individual electronic excitations.[18] Accordingly, the absorption spectrum of a system with two different (electronic or geometric) atoms should be the weighted addition of the characteristic spectrum of each particular atom. Therefore, we have made use of the XANES spectra to differentiate between the two mentioned possibilities. If Mn^{3+} and Mn^{4+} were present in the Mn-rich region (Ni^{3+} and Ni^{2+} in the Ni-rich region), the XANES spectra of intermediate compositions would be obtained by a weighted addition of the reference spectra with Mn^{3+} and Mn^{4+} (Ni^{3+} and Ni^{2+}). Obviously, the crystal structure of the references must be as similar as possible to the intermediate compounds. In our case, we have chosen the spectra of $LaNi_{0.5}Mn_{0.5}O_{3.05}$ as the reference for Mn^{4+} and Ni^{2+}. The references for Mn^{+3} and Ni^{+3} were $LaMnO_3$ and $LaNiO_3$, respectively. All of these references belong to the family of perovskite compounds with similar crystallographic structures.

Figure 8(a) compares the weighted addition of $\frac{1}{2}$ $LaNi_{0.5}Mn_{0.5}O_{3.05}$ and $\frac{1}{2}$ $LaNiO_3$ XANES spectra to the $LaNi_{0.75}Mn_{0.25}O_3$ experimental spectrum at the Ni *K* edge. The comparison shows similar features between experimental and calculated spectra but also important differences above the main edge and at the preedge region [indicated by arrows in Fig. 8(a)]. This result suggests that Ni atoms in $LaNi_{0.75}Mn_{0.25}O_3$ cannot be described as a mixture of Ni^{2+} (or the Ni present in $LaNi_{0.5}Mn_{0.5}O_3$) and Ni^{3+} (Ni in $LaNiO_3$). An intermediate-valence state seems to be a more suitable explanation. Moreover, this result discards a phase segregation of this compound in $LaNiO_3$ and $LaNi_{0.5}Mn_{0.5}O_3$ in agreement with a recent microscopic study.[11] Therefore,

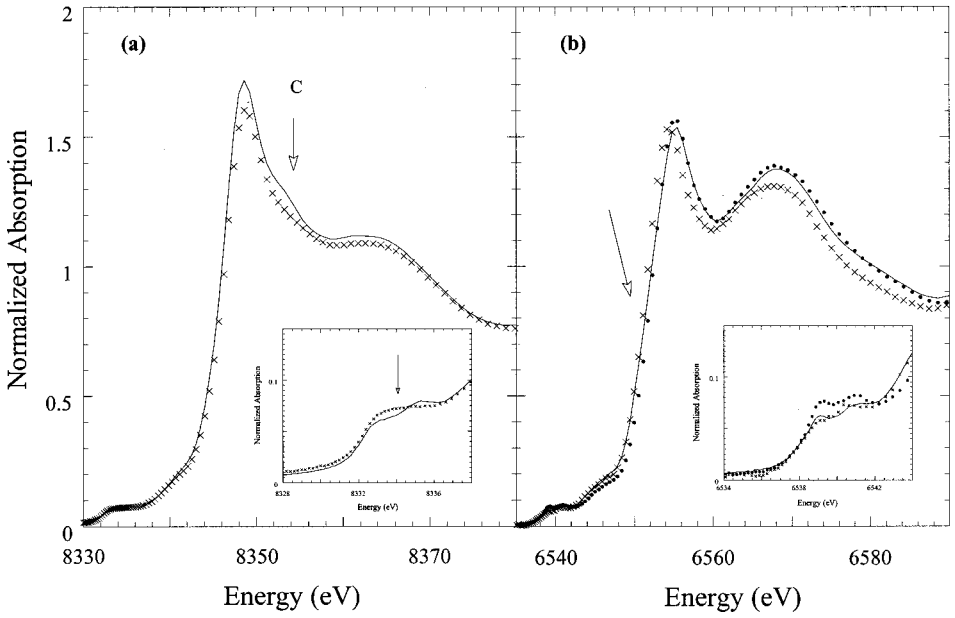

FIG. 8. (a) Ni *K*-edge XANES spectrum of $LaNi_{0.75}Mn_{0.25}O_3$ (crosses) compared to the spectrum obtained by the addition of $\frac{1}{2}$ $LaNiO_3$ and $\frac{1}{2}$ $LaNi_{0.5}Mn_{0.5}O_{3.05}$ spectra (line). (b) Mn *K*-edge XANES spectrum of $LaNi_{0.25}Mn_{0.75}O_{2.97}$ (crosses) and $LaNi_{0.25}Mn_{0.75}O_{3.09}$ (points) compared to the addition of $\frac{1}{2}$ $LaMnO_3$ and $\frac{1}{2}$ $LaNi_{0.5}Mn_{0.5}O_{3.05}$ spectra. Arrows indicate the main differences.

the large DW factor value observed in the EXAFS analysis of this sample (see Table II) must be ascribed to a local inhomogeneity instead of a phase segregation.

Figure 8(b) shows the results obtained for the Mn *K* edge in the Mn-rich region. Here the comparison is established between the experimental $LaNi_{0.25}Mn_{0.75}O_{2.97}$ spectrum and the following addition: $\frac{1}{2}$ $LaNi_{0.5}Mn_{0.5}O_{3.05}$ and $\frac{1}{2}$ $LaMnO_3$. This analysis is less conclusive for this compound, because simulated and experimental spectra are practically alike. However, the absorption edge for the experimental spectrum is sharper, in agreement with the presence of Mn in a unique oxidation state,[15,21] but the strong differences observed in the local structure around Mn atoms in the Mn-rich region (see Table II) induces us to think that in $LaNi_{1-x}Mn_xO_{3+\delta}$ ($x > 0.5$) samples the Mn ions are also in an intermediate-valence state.

The explanation of these results could be related to the high electronegativity of the Ni^{3+} cations. This ion polarizes the surrounding oxide anions (transforming itself practically into Ni^{2+}) and affects then the neighboring Mn-O bonds. Therefore, the holes could mainly be located at the Mn sublattice. The holes (electrons) localize at the Mn atoms (Ni atoms) in the Ni-rich region (Mn-rich region), but they are delocalized in the Mn-rich region (Ni-rich region) which gives rise to an intermediate valence. This is, of course, a naive approximation, because this system shows a strong mixing of Mn(Ni)-3*d* and O-2*p* states, as deduced from the preedge region of the absorption spectra. Moreover, one cannot discard the mixing of 3*d* states arising from different TM atoms. In summary, our results demonstrate that the most suitable ''ionic'' approximation to describe $LaNi_{0.5}Mn_{0.5}O_3$ would be $La_2Ni^{2+}Mn^{4+}O_6$.

The solid solution $LaNi_{1-x}Mn_xO_3$ cannot be considered as homovalent. The addition of Ni^{3+} to the $LaMnO_3$ would produce an oxidation of the Mn sublattice (coupled to the reduction of Ni^{3+}). In the same way, the incorporation of Mn^{3+} to $LaNiO_3$ would lead to a reduction of Ni^{3+} (and to an oxidation of Mn^{3+}). Moreover, these results do not seem to depend on synthetic details. Finally, it is noteworthy that the different spectroscopic measurements, EXAFS and XANES, on both atoms are consistent with this description.

ACKNOWLEDGMENTS

This work was supported by the Spanish C.I.C.Y.T. Project No. MAT99-0847. We thank ESRF and SRS for grating beam time.

*Corresponding author. Present address: I.C.M.A. Departamento de Física de la Materia Condensada, C.S.I.C.-Universidad de Zaragoza, Pedro Cerbuna, 12, 50009 Zaragoza, Spain. Fax:+34-976-761229. Email address: jgr@posta.unizar.es

[1] N. Tsuda, K. Nasu, A. Yanase, and K. Siratori, Electronic Conduction in Oxides, Springer Series in Solid State Sciences, Vol. 94 (Springer-Verlag, Heidelberg, 1991).

[2] J. M. D. Coey, M. Viret, and S. Von Molnar, Adv. Phys. **48**, 167 (1999).

[3] J. B. Goodenough, A. Wold, R. J. Arnott, and N. Menyuk, Phys. Rev. **124**, 373 (1961).

[4] G. J. Blasse, Phys. Chem. Solids **26**, 1969 (1965).

[5] K. Asai, H. Sekizawa, and S. J. Iida, J. Phys. Soc. Jpn. **47**, 1054 (1979).

[6] H. Fujiki and S. Nomura, J. Phys. Soc. Jpn. **23**, 648 (1967).

[7] N. Y. Vasanthacharya, P. Ganguly, J. B. Goodenough, and C. N. R. Rao, J. Phys. C **17**, 2745 (1984).

[8] D. D. Sarma, A. Chainani, S. R. Krishnakumar, E. Vescovo, C. Carbone, W. Eberhardt, O. Rader, Ch. Jung, Ch. Hellwing, W. Gudat, H. Skrikanth, and A. K. Raychauduri, Phys. Rev. Lett. **80**, 4004 (1998).

[9] J.-H. Park, S.-W. Cheong, and C. T. Chen, Phys. Rev. B **55**, 11 072 (1997).

[10] C. Zener, Phys. Rev. **82**, 403 (1951).

[11] J. Blasco, J. García, M. C. Sánchez, A. Larrea, J. Campo, and G. Subías, J. Phys.: Condens. Matter **13**, L729 (2001).
[12] J. Blasco, M. C. Sánchez, J. Pérez-Cacho, J. García, G. Subías, and J. Campo, J. Phys. Chem. Solids **63**, 781 (2002).
[13] A. Wold and R. J. Arnott, J. Phys. Chem. Solids **9**, 176 (1959).
[14] J. García, G. Subías, M. G. Proietti, H. Renevier, Y. Joly, J. L. Hodeau, J. Blasco, M. C. Sanchez, and J. F. Berar, Phys. Rev. Lett. **85**, 578 (2000); J. García, G. Subías, M. G. Proietti, J. Blasco, H. Renevier, J. L. Hodeau, and Y. Joly, Phys. Rev. B **63**, 054110 (2001).
[15] J. García, M. C. Sánchez, G. Subías, and J. Blasco, J. Phys.: Condens. Matter **13**, 3229 (2001); G. Subías, J. García, M. G. Proietti, and J. Blasco, Phys. Rev. B **56**, 8183 (1997); J. García, M. C. Sánchez, J. Blasco, G. Subías, and M. G. Proietti, J. Phys.: Condens. Matter **13**, 3242 (2001).
[16] J. Blasco, M. Castro, and J. García, J. Phys.: Condens. Matter **6**, 5875 (1994).
[17] C. Ritter, M. R. Ibarra, J. M. De Teresa, P. A. Algarabel, C. Marquina, J. Blasco, J. García, S. Oseroff, and S-W. Cheong, Phys. Rev. B **56**, 8902 (1997).
[18] D. C. Koningsberger and R. Prins, *X-Ray Absorption Techniques of EXAFS, SEXAFS and XANES* (Wiley, New York, 1988).
[19] J. J. Rehr, J. Mustre de Leon, S. I. Zabinsky, and R. C. Albers, J. Am. Chem. Soc. **113**, 5135 (1991).
[20] G. Subías, J. García, J. Blasco, and M. G. Proietti, Phys. Rev. B **58**, 9287 (1998).
[21] C. H. Booth, F. Bridges, G. J. Snyder, and T. H. Geballe, Phys. Rev. B **54**, R15 606 (1996).
[22] R. D. Shannon, Acta Crystallogr., Sect. A: Cryst. Phys., Diffr., Theor. Gen. Crystallogr. **32**, 751 (1976).
[23] J. García, J. Blasco, M. G. Proietti, and M. Benfatto, Phys. Rev. B **52**, 15 823 (1995).
[24] K. Hong, Y-U. Kwon, D-K. Han, J-S. Lee, and S-H. Kim, Chem. Mater. **11**, 1921 (1999).
[25] M. Abbate, F. M. F. de Groot, J. C. Fuggle, A. Fujimori, O. Strebel, F. López, M. Dombke, G. Kaindl, G. A. Sawatzky, M. Takano, Y. Takeda, H. Eisaki, and S. Uchida, Phys. Rev. B **46**, 4511 (1992).
[26] Y. Moritomo, Sh. Xu, A. Machida, T. Akimoto, E. Nishibori, M. Takata, and M. Sakata, Phys. Rev. B **61**, R7827 (2000); F. S. Galasso, *Structure, Properties and Preparation of Perovskite-Type Compounds*, International Series of Monographs in Solid State Physics (Pergamon, New York, 1969).